JOURNAL OF BASIC SCIENCE AND ENGINEERING

AUTOMATED FEATURE EXTRACTION AND CLASSIFICATION OF COVID-19 CHEST X-RAY IMAGES USING CONVOLUTIONAL NEURAL NETWORKS AND XGBOOST ALGORITHMS

N. Sundaravalli [1] & Dr. R. Vidyabanu [2]

1. Research Scholar, PG & Research Department Of Computer Science,
L.R.G Govt. Arts College For Women, Tirupur – 4.
shinisuba99@yahoo.com

2. Assistant Professor, PG & Research Department Of Computer Science,
L.R.G Govt. Arts College For Women, Tirupur-4.
vidhyabanu@yahoo.com

Abstract: *In the upgrowing astounding development of the medical epoch, people are trying and fighting several diseases to extend their life. Ever since the arrival of covid –19 (SARS-CoV2) epidemic health crisis took over the world, was a major challenge to the global healthcare centre, to prevent human efforts of disease containment from being overwhelmed, we need tools that can streamline the diagnosis, surveillance, and treatment at right time and manage it properly. the detection of COVID-19 using the conventional method is time-consuming, not very accurate, and error-prone. During this period, the alternate solution of the medical X-ray image plays an important role in diagnosing COVID-19 patients effectively. This current research work takes the dataset of COVID-19-affected chest X-rays and proposes a Deep Learning (DL)-based approach. The images are pre-processed using Median Filter (MF) and Contrast-Limited Adaptive Histogram Equalization (CLAHE). The features are extracted using the Gray Level Co-occurrence Matrix (GLCM) and Convolutional Neural Network (CNN). The images are classified using Random Forest (RF) and eXtreme Gradient Boosting (XGBoost). Experimental results show the efficiency of the proposed model CNN_XGBoost offers better results in terms of Accuracy, Precision, Recall and F-Measure in contrast to RF, CNN and CNN_RF.*

Keywords: *Covid-19, Chest X-Ray images, Median Filter, Contrast-Limited Adaptive Histogram Equalization (CLAHE), Gray Level Co-occurrence Matrix (GLCM), Convolutional Neural Network (CNN), Random Forest (RF), eXtreme Gradient Boosting (XGBoost).*

1. INTRODUCTION

1.1 COVID-19

Coronavirus disease 2019 (COVID-19) or Severe acute respiratory syndrome coronavirus 2 (SARS-CoV-2) is a highly transmittable respiratory disease caused by a novel coronavirus, which threatens human life. The virus was first identified in the city of Wuhan, Hubei, China, in December 2019 and called as 2019 novel coronavirus (2019-nCoV), and human coronavirus 2019 (HCoV-19 or hCoV-19).[6][35][36]. The World Health Organization designated the

outbreak a public health emergency of international concern from January 30, 2020, to May 5, 2023.[7]. The scientists believe the SARS-CoV-2 virus entered into human populations through natural zoonosis, similar to the SARS-CoV-1 and Middle East respiratory syndrome coronavirus (MERS-CoV) outbreaks, and the disease quickly spread worldwide, consistent with other pandemics in human history.

1.2. Symptoms

Over this period, People with covid 19 are symptomatic, pre-symptomatic & asymptamatic infection. The Asymptamatic person had no symptoms throughout the diseases course time, less carrier but high transmitter than others. [7][39] The symptoms in people with the covid 19 are similar to those of the influenza-like illness such as fever, headache, body pain, cold, and cough. The disease can be mild, moderate, or severe and recover without requiring special treatment. However, some will become seriously ill and require medical attention. Hence isolation and quarantine are necessary to prevent the spread of the virus. It can be dangerous because it can lead to cytokine storm, severe respiratory illness with respiratory failure, pneumonia, acute respiratory distress syndrome, liver injury, acute cardiac injury, disseminated intravascular coagulation, kidney failure, secondary infection, bleeding disorders, multiorgan failure, and septic shock. [37]

1.3 The global communication challenge and scientific collaboration

According to the World Health Organization (WHO) COVID-19 Dashboard (https://covid19.who.int/), this pandemic has plagued the world, resulting in over 636 million cases and 6.6 million fatalities to date.[35]. The Infectious disease outbreaks have posed a new challenge for epidemiologists keenly expanding the research with other fields, such as physics, mathematics, computer science, and network science like unprecedented scientific collaboration worldwide, who have been contributing their ideas and expertise breakthrough discoveries can be accelerated and insights broadened to fight against the disease.

Although, Conventional molecular & serological detection of COVID19 using reverse transcription-polymerase chain reaction (RT-PCR) is time-consuming and error-prone, so some other alternative time and cost-effective method is needed to diagnose the disease accurately.[1][8]. Here Computer-Aided Medical Image plays an important role in effectively

Vol. 21, No. 1, (2024)
ISSN: 1005-0930

complementing the conventional one to analyze the image quality in decision-making. The images are generally infected by noise which degrades the image quality and delays the result in decision making. Hence, it becomes necessary to enhance the image quality by de-noising the image through applying image processing algorithms. [2][4] [38].

1.4 The Present work

The current paper focuses on image de-noising of COVID-19-affected chest X-rays and proposed Deep Learning (DL) and Machine Learning or a hybrid-based approach are employed for feature extraction and classification process.[3] [5]. The remaining sections of this work are well organized as follows, Section II contains, a review related work of this study, Section III is concerned with the images are pre-processed using Median Filter (MF) and Contrast Limited Adaptive Histogram Equalization (CLAHE). Section IV resolves the features extracted using Gray Level Co-occurrence Matrix (GLCM) and the proposed Convolutional Neural Network (CNN). Section V expounds, medical images are classified using Random Forest (RF) and proposed eXtreme Gradient Boosting (XGBoost). Section VI Experimental Result and finally, Section VII concludes the study.

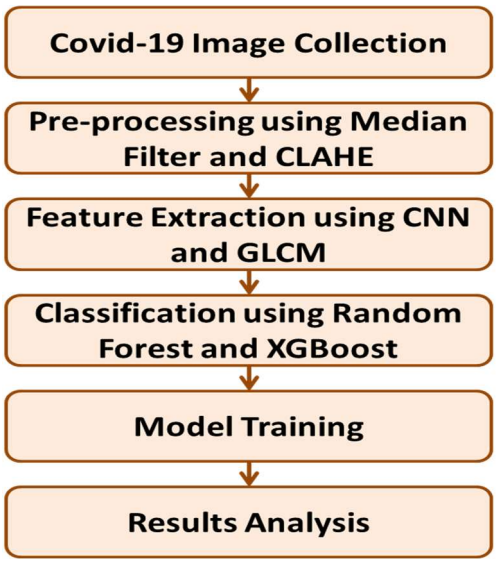

Figure 1: Proposed Framework

Vol. 21, No. 1, (2024)
ISSN: 1005-0930

2. RELATED WORK

Joaquin (2020) [19] have designed ResNet50 based deep Transfer Learning (TL) scheme and have shown improved accuracy for a dataset including 339 images for training as well as testing.

Likewise, Heidari *et. al.,* (2020) [20] have applied pre-processing for identifying Covid-19 by using X-ray images. Images are classified using Convolutional Neural Network (CNN) and diaphragm areas in images are removed. Feature extraction is performed to enhance classification accuracy of CNN model used.

Wang *et. al., (2020)* [21] have propounded several pre-trained DL models wherein Xception model shows a moderately ideal impact with improved accuracy. Dataset consists of 1102 X-ray chest images of fit patients along with patients suffering from Covid-19 arbitrarily split into training and test sets. Hence, advancing DL to identify lung images with Covid-19 is essential.

This has motivated conducting a relative analysis of advanced techniques for X-ray as well as CT images to deal with Deep Neural Network (DNN) structure employed in the field to examine merits as well as demerits of them, to examine most appropriate ones by using improved datasets built from public sources.

Lately, COVID-19 pneumonia identification schemes depending on DL are defined by some groups. Alshazly *et. al.,* (2021) [22] have used deep CNN frameworks on CT images to identify the disease with increased accuracy, sensitivity and precision correspondingly.

Using CNN-based T-BiLSTM (CNN-TL-BiLSTM) for diagnosing Covid-19 using CT images, Aslan *et. al.,* (2021) [23] have performed lung segmentation to improve success rate. Features are chosen by segmentation.

Bhattacharyya *et. al.,* (2022) [24] have proposed a method for Covid-19 detection which includes 3-steps. Initially, the X-ray images are segmented using Conditional Generative Adversarial Network (C-GAN) for getting lung images. The segmented images are sent to a pipeline that joins key point extraction techniques and DNN for feature extraction. The images are classified using numerous ML models. The proposed scheme offers improved classification accuracy using VGG-19 model linked with Binary Robust Invariant Scalable Key-points (BRISK) algorithm.

Vol. 21, No. 1, (2024)
ISSN: 1005-0930

Salama & Aly (2022) [25] have used ResNet50 as well as VGG16 models to classify CT images of lung. These models are combined with U-Net to segment images before classification. Furthermore, Image Size Dependent Normalization Technique (ISDNT) along with Wiener filter is used as for pre-processing to improve images and suppress noise. TL and data augmentation schemes are used for handling deficient lung images, thus avoiding overfitting of deep models. The proposed model offers improved accuracy, area under ROC curve, sensitivity, precision and F1-score with reduced computational time.

Aslani & Jacob (2023) [26] offers a review of DL-based AI schemes using radiography as well as CT. Several papers are published using 2D/3D DCNNs joint with TL for detecting Covid-19 detection. The limitations of proposed schemes are also detailed.

Constantinou *et. al.,* (2023) [27] have used DL models for identifying Covid-19 from X-ray images. The significance and capability of DL models are highlighted. ResNet50, ResNet101, DenseNet169, DenseNet121 along with InceptionV3 which employs TL are applied on CXR images of Covid-19. They were assessed on unknown data. The models offer acceptable performance with ResNet101 offering improved Precision, Accuracy and Recall.

3. PRE-PROCESSING

Image preprocessing is the process of manipulating raw image data into a usable format, and used to abolish unwanted distortions and improve exact qualities essential for computer vision applications. In this work, Images are pre-processed using Median Filter (MF) and Enhanced the image using Contrast Limited Adaptive Histogram Equalization (CLAHE).

3.1 Median Filter (MF)

Median Filter (MF) is used for removing noise from an image. This non-linear digital filtering mechanism used for removing noise from image. It is efficient in eliminating impulse noise in image. Noise reduction deals with pre-processing for improving outcomes of processing. It is employed in Digital Image Processing (DIP) wherein under particular conditions, it preserves edges when eliminating noise.

The key idea of MF is to move through each signal, replacing every entry with median of adjoining entries. Neighbours are represented as ‘window’ that slides through the entries over

Vol. 21, No. 1, (2024)
ISSN: 1005-0930

whole signal. For 1-D signals, window is initial few preceding and ensuing entries, however for 2-D (high dimensions) data, window should comprise of entries in a specified radius or ellipsoidal region.

The principle is to substitute gray level of every pixel by gray level's median in pixel's neighbourhood rather than using average function. Kernel size and pixel values are specified, and level of median is determined. In case kernel covers uniform amount of pixels, mean of median values is employed. Before performing median filtering, zeros are to be padded round bout row as well as column edges. Edge distortion is included in image border.

Local intensity distributions are considered and an image conforming to set of median values is generated. It offers improved impulse noise suppression. It includes a 3 x 3 kernel for filtering impulse noise. The image is smoothed, and high-frequency information is lessened. A kernel of increased size is not suitable as for a huge collection of pixels this value diverges from value of pixel.

Median Filtering:

W - Width

H - Height

Win - Window

Assign outputPixel [W] [H]

Assign Win [W × H]

$\text{Edge}_\text{X} = \left(\frac{\text{W}}{2}\right).\text{rounded down}$

$\text{Edge}_\text{Y} = \left(\frac{\text{H}}{2}\right).\text{rounded down}$

for $(\text{X} = \text{Edge}_\text{X}\ \text{to}\ \text{W} - \text{Edge}_\text{X})$

for$(\text{Y} = \text{Edge}_\text{Y}\ \text{to}\ \text{H} = - \text{Edge}_\text{Y})$

i = 0

for $(\text{f}_x = 0\ \text{to}\ \text{W})$

for $(\text{f}_y = 0\ \text{to}\ \text{H})$

$\text{Win}[\text{i}] = \text{inputPixel}\ [\text{X} + \text{f}_x - \text{Edge}_\text{X}]\ [\text{Y} + \text{f}_y - \text{Edge}_\text{Y}]$

i+=1

Vol. 21, No. 1, (2024)
ISSN: 1005-0930

Organise entries in the Win[]

$$\text{outputPixel[X][Y]} = \text{Win}\left[\text{W} \times \frac{\text{H}}{2}\right]$$

Histogram array is initialised to zero and image is scanned, producing an image in Q-space. For each region, histogram consisting of intensity values is built. Median is determined and points present in histogram array which are incremented are set to zero. This feature removes the demand for clearing the histogram and saves computation. Extreme intensity values are found and search for median is limited to the range. When median is found, only a scan through distribution is needed, as total area is identified in advance. Pixel intensity sorting operations are involved.

3.2 Contrast Limited Adaptive Histogram Equalization (CLAHE)

CLAHE is developed for enhancing images with reduced contrast [28]. Histogram clipping takes place at the limit defined by user limit amplification. Level of clipping takes control of the amount of noise in histogram that must be smoothed and the contrast that should be increased. Colour version of CLAHE is used with clipping set to 2.0 and grid size of 8 × 8.

Steps:

- ✓ Convert the RGB image into LAB image
- ✓ Apply CLAHE to 'L' channel
- ✓ Merge the improved 'L' channel with 'A' as well as 'B' to obtain enriched LAB image
- ✓ Convert the improved LAB image into enriched RGB image
- ✓ Resize images into ones of size 224 × 224 × 3 as images are of different resolutions
- ✓ Perform normalization on every image

CLAHE varies from ordinary AHE in limiting contrast. To deal with the challenge of noise amplification, CLAHE employs a clipping limit. Before Cumulative Distribution Function (CDF) is computed, Amplification is limited by clipping histogram at a pre-determined value. It splits an input image into non-overlying regions called blocks or tiles.

Vol. 21, No. 1, (2024)
ISSN: 1005-0930

It is defined using 2 factors namely, Block Size (BS) and Clip Limit (CL). These parameters chiefly manage enhanced image quality. As CL is improved, image is made brighter as the image has reduced intensity and increased CL making histogram flatter.

With increase in BS, the dynamic range and image contrast increase. The parameters found at point of Maximum Entropy (ME) curvature offer subjectively better image quality.

4. FEATURE EXTRACTION

Feature extraction is the process of identifying and selecting the most important information or characteristics from a data set, the goal is to make complicated information simpler. In this paper, features are extracted using Convolutional Neural Networks **(**CNN) and Gray Level Co-occurrence Matrix (GLCM).

4.1 Convolutional Neural Networks (CNN)

CNNs offer better performance which considers image, speech as well as audio as input. They include the following layers:

- ✓ Convolutional
- ✓ Pooling
- ✓ Fully-connected (FC)

The convolutional layer is the first layer that is followed by added pooling or convolutional layers with FC layer as last layer. The complexity increases with inclusion of more number of layers classifying better parts of image. Former layers emphases on simple characteristics like colours as well as edges.

As data of image is passed through all layers, it commences recognising huge elements or shapes until it lastly finds the envisioned object.

- ✓ **Convolutional Layer:** It forms the base and most of the computation occurs here. It demands input data, Feature Map (FM) and filter. Colour image is taken as input. The input has 3 dimensions including height, width as well as depth that relate to Red Green Blue (RGB) in an image. A feature identifier called kernel that moves across images' receptive fields, determining whether feature is present or not. The Filter is of size 3x3

Vol. 21, No. 1, (2024)
ISSN: 1005-0930

matrix. The receptive field's size is found. Filter and dot product are applied amid input pixels as well as filter. Filter moves by strides, reiterating until kernel moves through whole image. Output from sequence of dot products of input and filter is a FM, feature or activation map.

- ✓ **Pooling Layer:** Down sampling performs dimensionality lessening, dropping the amount of input parameters. Compared to convolutional layer, the pooling layer sweeps a filter over whole input. Weights are not included in the filter. Kernel aggregates values in receptive field inhabiting output array. It includes 2 pooling layers.
  - **Max-Pooling (MP):** As filter is applied on input, it chooses pixel with increased value to forward to output array. This scheme can be used frequently in contrast to average pooling.
  - **Average pooling:** As filter moves over input, it finds average in receptive field to forward to output array.

- ✓ **Fully-Connected (FC) Layer:** Pixels of image are not linked to Output Layer (OL) in partly associated layers. Nevertheless in FC layer, every node in OL links to node in former layer. Classification is depending on features taken through former layers and diverse filters. As convolutional as well as pooling layers employ ReLu functions, FC layers influence Softmax activation function to categorize input suitably generating a probability of 0 to 1.

Extracting features by image processing schemes are inaccurate and challenging. As complex features are involve in Covid-19 CT images, a deep Convolutional Neural Network (CNN) for determining 100 noticeable features.

Batch normalization and MP layer follow convolution layers. After 100 epochs, model learns classification parameters. Learning rate is set to 0.001 during training. Optimisation is done using 'Adam' and dropout probability of 0.50 is used for obtaining more generalized outcomes.

Vol. 21, No. 1, (2024)
ISSN: 1005-0930

Once learning is done, dataset is given to trained CNN model. 100 prominent features of each image are extracted from last but previous dense layer including 100 neurons.

4.2 Gray Level Co-occurrence Matrix (GLCM)

GLCM is a statistical technique that examines texture by considering spatial association of pixels. It is also called gray-level spatial dependence matrix. The functions describe image texture by determining how frequently pixel pairs with particular values and in particular spatial association are seen in the image. GLCM is formed and statistical measures are extracted from the matrix. Information about pixels' spatial relationships in an image is not offered by texture filter functions.

GLCM is used for distinguishing image texture by computing existence of pixel pairs with a value in a particular direction. Statistical features are extracted including autocorrelation, shade and prominence, contrast, variance, information measure of Correlation-1 and Correlation-2, difference normalized, moment normalized, difference moment and energy, maximum probability, entropy etc.,

For a grey-level image (I), the Co-occurrence Matrix (C) is used for determining how often the pixel pairs with particular value as well as offset present in image.

- Offset $(\Delta X, \Delta Y)$ is a location operator which may be added to images without edge effects.
- For a particular offset, image with 'P' pixels produce 'P × P' Co-occurrence matrix
- The $(i,j)^{th}$ value of 'C' gives number of times that 'i^{th}' and 'j^{th}' pixel in relation given by offset

For image with 'P' pixels, 'C' is defined on an $n \times m$ image (I) parameterized by $(\Delta X, \Delta Y)$ as:

$$C_{\Delta X,\Delta Y}(i,j) = \sum_{X=1}^{n} \sum_{Y=1}^{m} \begin{cases} 1, \text{if } I(X,Y) = i \text{ and } I(X+\Delta X, Y+\Delta Y) = j \\ 0, \text{Otherwise} \end{cases} \quad (1)$$

Where,

'i' & 'j' - Values of pixels

Vol. 21, No. 1, (2024)
ISSN: 1005-0930

X & Y - Spatial locations in 'I'

$(\Delta X, \Delta Y)$ - Spatial association for which matrix is found

$I(X, Y)$ - Pixel at (X, Y)

GLCM is capable of extracting low-level features. So there are chances for skipping several features. To handle this situation, in GLCM-CNN, features are extracted using GLCM followed by extraction of high level features using CNN. Finally, features points over relevant features are obtained.

5. CLASSIFICATION

In this section Images are classified using Random Forest (RF) and proposed XGBoost.

5.1 Random Forest (RF)

Random Forest (RF) is based on supervised learning which forms a 'forest' from a collection of Decision Trees (DTs) that are normally trained by using 'bagging'. They are fully automated ML techniques. Combining numerous learning models enhances the outcome.

It does not need preparation of data or modelling expertise. Fundamental block of RF is DT used as classification as well as Regression Trees (RTs). Models are built by dividing data amid diverse DTs and taking mean of DT predictions as response.

RF includes several random DTs. Two kinds of randomness are constructed into trees. Every tree is constructed on an arbitrary sample from data. At every node, a subcategory of features is arbitrarily chosen to produce the finest split.

A random subgroup of features is considered for node splitting. Random trees can be produced by using random thresholds for every feature instead of searching for best thresholds.

An understanding of ensemble technique is essential. Ensemble involves merging numerous models. A group of models is used for making predictions rather than a single model. Ensemble involves 2 kinds of techniques:

RF is used in classification as well as regression problems. It forms DTs on diverse samples and takes majority vote for classification and average for regression. RF handles dataset including

Vol. 21, No. 1, (2024)
ISSN: 1005-0930

continuous variables for regression as well as categorical variables for classification. It offers improved classification outcomes.

During training, several DTs are formed and output is given as classes or average of singular tree's estimate [29]. They are capable of handling the overfitting problem seen in training data for DTs [30].

5.2 eXtreme Gradient Boosting (XGBoost)

XGBoost is optimised form of Gradient Boosting (GB) algorithm. Several modifications are made and high-performance classifier is obtained. The most significant algorithm features include increased prognostic power, avoid over-learning and handle blank data rapidly. It is considered as best DT-based algorithms. Several trees or models called weak learners are built sequentially [31]. Every model tries learning from errors of former one, thus offering enhanced and precise model. It is an implementation of GB DTs. The models are used in several Kaggle competitions.

DTs are sequentially generated. Weights play a significant role and are allocated to every variable that are fed into DT that forecasts outcomes. The variable weights which are wrongly predicted are increased and the variables are fed to second DT. The classifiers or predictors are then ensembled to obtain a robust and accurate model. It works on regression, ranking, classification and prediction problems.

Prediction scores of the DTs are then summed up. Two trees complement one other. Mathematically,

$$\breve{Y}_i = \sum_{k=1}^{K} f_k(k_i), f_k \in F$$

Where,

K - Quantity of trees

f - F's Functional space

F - Set of CARTs

The objective function is given by:

$$Obj(\theta) = \sum_i^n l\left(\breve{Y}_i, Y_i\right) + \sum_{k=1}^{K} \varphi(f_k)$$

Where,

Vol. 21, No. 1, (2024)
ISSN: 1005-0930

$\sum_{i}^{n} l(\tilde{Y}_i, Y_i)$ - Loss function

$\sum_{k=1}^{K} \varphi(f_k)$ - Regularization parameter

Trees are sequentially constructed and the tree focuses on reducing errors of former tree. Every tree acquires knowledge from the predecessors and modifies the remaining errors. The tree which grows in sequence learns from update version of residuals.

The base learners are weak wherein, bias is increased and prognostic power is improved when compared to arbitrary guessing. Every weak learner offers some essential information for performing prediction, permitting the boosting scheme to generate a strong learner by efficiently joining weak learners. The concluding strong learner reduces bias as well as variance.

Contrary to bagging schemes like RF, wherein trees grow to maximum extent, boosting uses trees with less number of splits. These small trees that are not deep are extremely understandable. Factors including amount of trees, learning rate of GB, and tree depth can be ideally chosen using validation schemes like k-fold Cross Validation (CV). Increased amount of trees cause overfitting. Hence, it is essential to carefully select stopping criteria for boosting.

GB ensemble scheme includes the following steps.

- A model (f_0) is used for predicting target (y). It is connected with residual ($y - f_0$).
- Model (h_1) is set to residuals from former step
- 'f_0' and 'h_1' are joined to generate 'f_1', boosted form of 'f_0'. The Mean Square Error (MSE) from 'f_1' will be less than that from 'f_0'.

$$f_1(x) = f_0(x) + h_1(x) \qquad (2)$$

To enhance performance of 'f_1', residuals of 'f_1' are modelled to form 'f_2'.

$$f_2(x) = f_1(x) + h_2(x) \qquad (3)$$

This involves 'm' iterations till residuals are reduced to the maximum extent possible.

$$f_m(x) = f_{m-1}(x) + h_m(x) \qquad (4)$$

The additional learners do not disrupt functions generated in former steps. Rather, they report information to reduce errors.

Initially, the model is initialized as '$f_0(x)$' which reduces loss function or MSE.

$$f_0(x) = \operatorname{argmin}_{\alpha} \sum_{i=1}^{n} L(y_i, \alpha) \qquad (5)$$

Vol. 21, No. 1, (2024)
ISSN: 1005-0930

$$\text{argmin}_{\alpha} \sum_{i=1}^{n} L(y_i, \alpha) = \text{argmin}_{\alpha} \sum_{i=1}^{n} (y_i - \alpha)^2 \quad (6)$$

By considering the first differential of the equation based on 'α', the function shows a reduced value at the mean $\left(\frac{\sum_{i=1}^{n} y_i}{n}\right)$. The model is initiated as follows:

$$f_0(x) = \frac{\sum_{i=1}^{n} y_i}{n} \quad (7)$$

'$f_0(x)$' offers predictions from initial stage of the model. The residual error for every instance is given by $(y_i - f_0(x))$.

6. RESULTS AND DISCUSSION

The performance of the existing and the proposed schemes are analysed by applying them on dataset from Kaggle. The training and testing datasets were obtained by splitting the dataset into 70% and 30% ratio.

The database for Covid-19 includes X-ray images of positive, normal and pneumonia images released in stages. Initially, 219, 1341 and 1345 images were included in each category respectively. In next update, Covid-19 class was updated with 1200 images, followed by 3616,

Vol. 21, No. 1, (2024)
ISSN: 1005-0930

192 and 1345 cases belonging to the 3 categories along with 6012 Lung Opacity images.

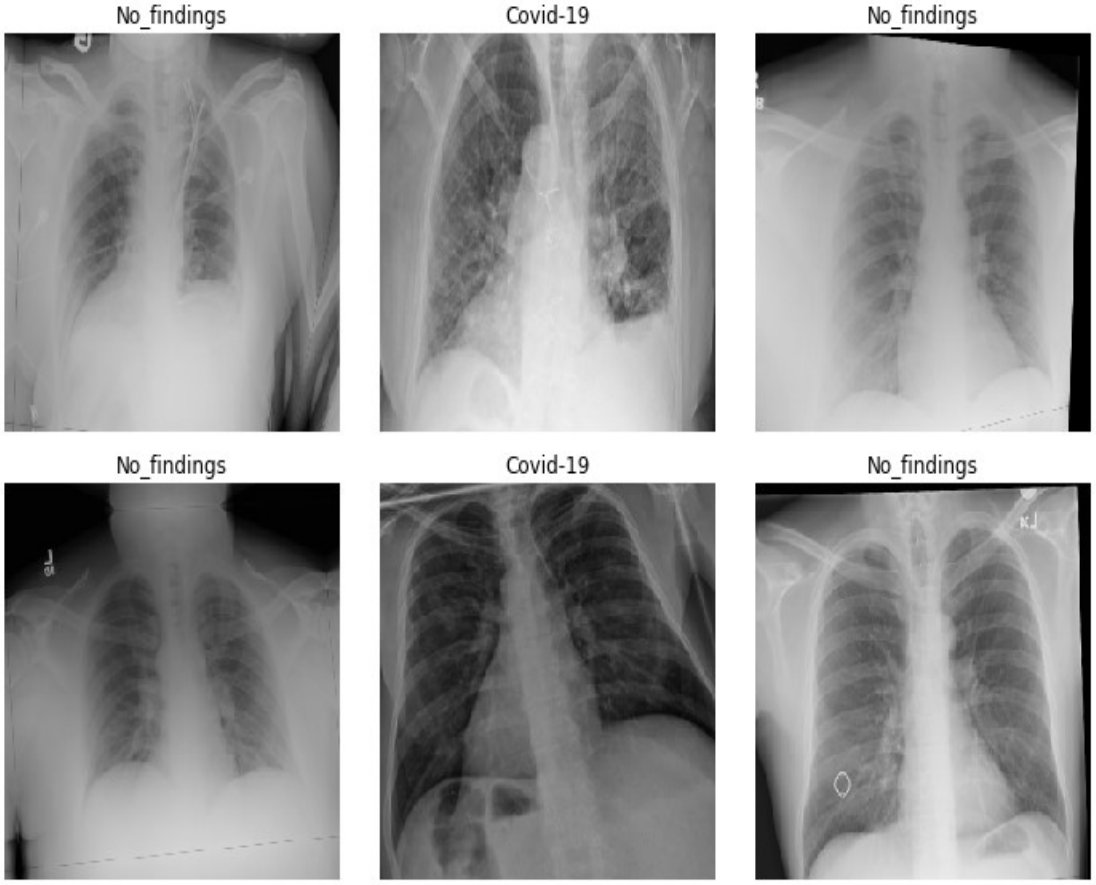

Figure 2: Sample Images

Vol. 21, No. 1, (2024)
ISSN: 1005-0930

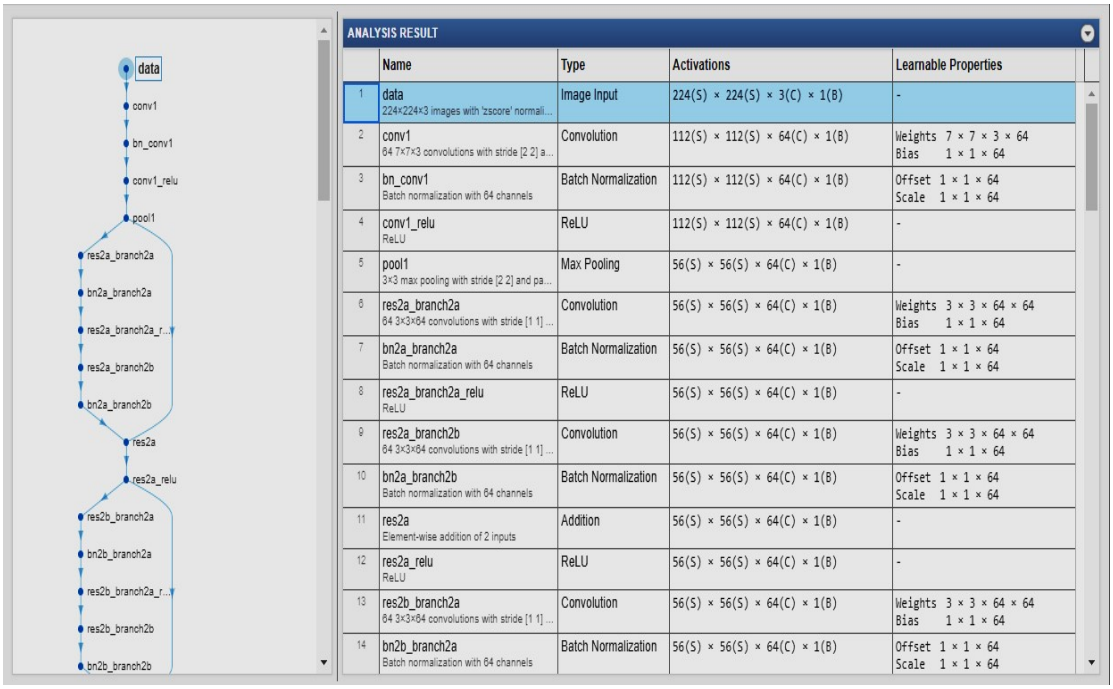

ANALYSIS RESULT

	Name	Type	Activations	Learnable Properties
1	data 224×224×3 images with 'zscore' normali...	Image Input	224(S) × 224(S) × 3(C) × 1(B)	-
2	conv1 64 7×7×3 convolutions with stride [2 2] a...	Convolution	112(S) × 112(S) × 64(C) × 1(B)	Weights 7 × 7 × 3 × 64 Bias 1 × 1 × 64
3	bn_conv1 Batch normalization with 64 channels	Batch Normalization	112(S) × 112(S) × 64(C) × 1(B)	Offset 1 × 1 × 64 Scale 1 × 1 × 64
4	conv1_relu ReLU	ReLU	112(S) × 112(S) × 64(C) × 1(B)	-
5	pool1 3×3 max pooling with stride [2 2] and pa...	Max Pooling	56(S) × 56(S) × 64(C) × 1(B)	-
6	res2a_branch2a 64 3×3×64 convolutions with stride [1 1] ...	Convolution	56(S) × 56(S) × 64(C) × 1(B)	Weights 3 × 3 × 64 × 64 Bias 1 × 1 × 64
7	bn2a_branch2a Batch normalization with 64 channels	Batch Normalization	56(S) × 56(S) × 64(C) × 1(B)	Offset 1 × 1 × 64 Scale 1 × 1 × 64
8	res2a_branch2a_relu ReLU	ReLU	56(S) × 56(S) × 64(C) × 1(B)	-
9	res2a_branch2b 64 3×3×64 convolutions with stride [1 1] ...	Convolution	56(S) × 56(S) × 64(C) × 1(B)	Weights 3 × 3 × 64 × 64 Bias 1 × 1 × 64
10	bn2a_branch2b Batch normalization with 64 channels	Batch Normalization	56(S) × 56(S) × 64(C) × 1(B)	Offset 1 × 1 × 64 Scale 1 × 1 × 64
11	res2a Element-wise addition of 2 inputs	Addition	56(S) × 56(S) × 64(C) × 1(B)	-
12	res2a_relu ReLU	ReLU	56(S) × 56(S) × 64(C) × 1(B)	-
13	res2b_branch2a 64 3×3×64 convolutions with stride [1 1] ...	Convolution	56(S) × 56(S) × 64(C) × 1(B)	Weights 3 × 3 × 64 × 64 Bias 1 × 1 × 64
14	bn2b_branch2a Batch normalization with 64 channels	Batch Normalization	56(S) × 56(S) × 64(C) × 1(B)	Offset 1 × 1 × 64 Scale 1 × 1 × 64

Figure 3: Architecture of CNN model Figure 2 shows a set of sample images while Figure 3 shows the framework of CNN model.

Figure 4 shows the Confusion Matrix of overall dataset.

Figure 5 shows the actual and predicted normal and Covid-19 sample images

```
125 122 0.976
[[ 21   3]
 [  0 101]]
              precision    recall  f1-score   support

    Covid-19       1.00      0.88      0.93        24
  No_findings      0.97      1.00      0.99       101

   micro avg       0.98      0.98      0.98       125
   macro avg       0.99      0.94      0.96       125
weighted avg       0.98      0.98      0.98       125
```


Vol. 21, No. 1, (2024)
ISSN: 1005-0930

Figure 4: Confusion Matrix of Overall Dataset

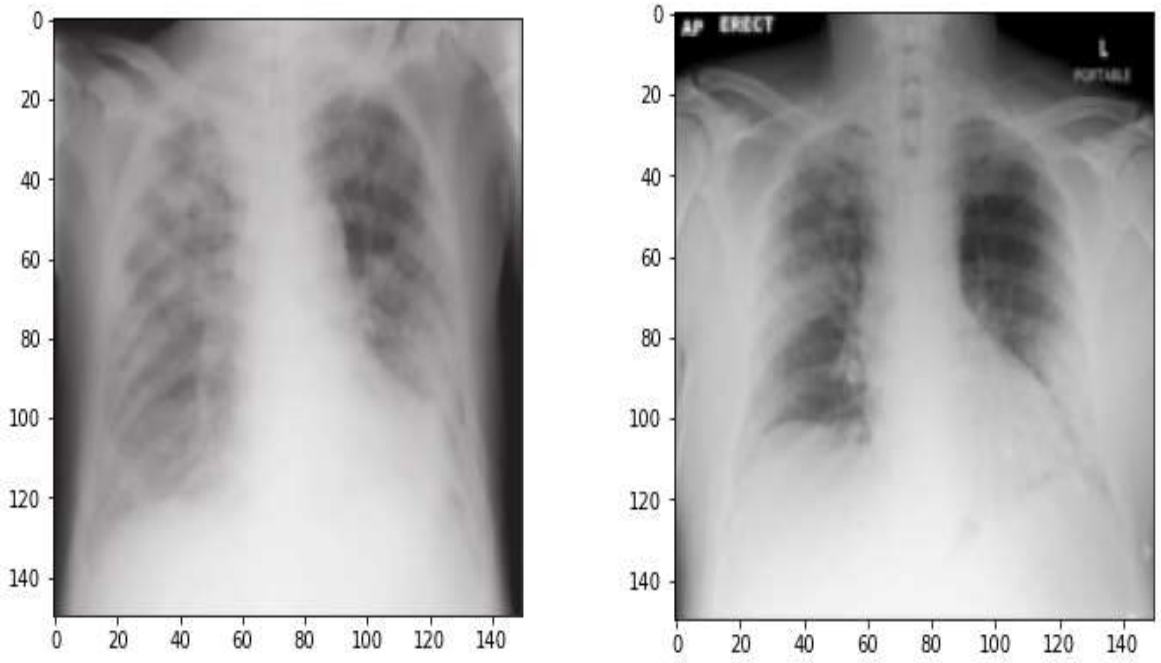

Figure 5: (a) Actual and Predicted Normal (b) Actual and Predicted Covid-19 Sample

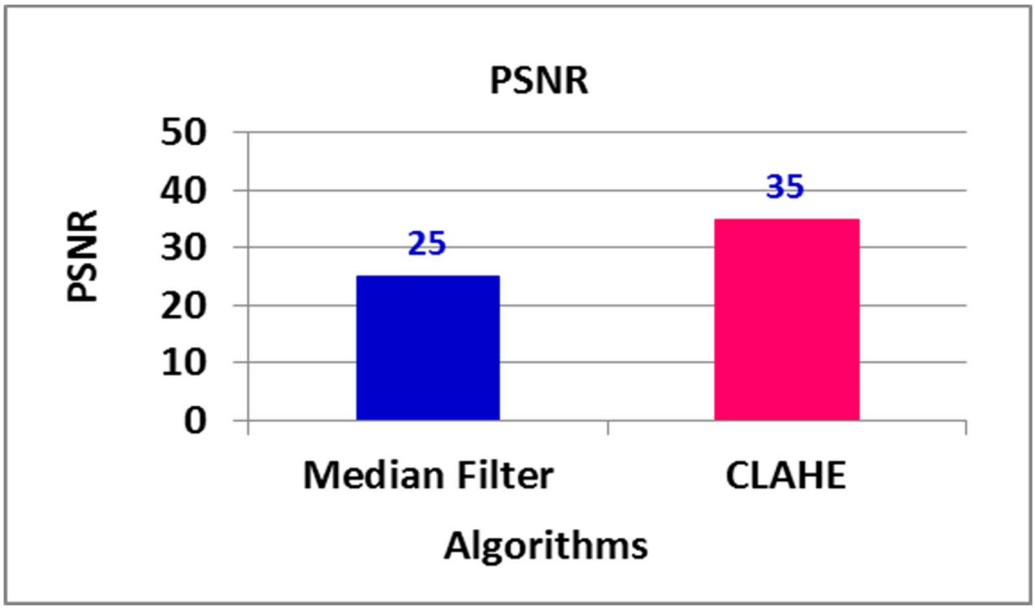

Vol. 21, No. 1, (2024)
ISSN: 1005-0930

Figure 6: Peak signal-to-noise ratio (PSNR) Figure 6 shows the PSNR. It is seen that CLAHE offers 40% better PSNR in contrast to Median Filter. Figure 7 shows the MSE. It is seen that CLAHE offers 2.7 times reduced MSE when compared to Median Filter.

Figure 8 shows the Structural Similarity Index (SSI). It is seen that CLAHE offers 11.4% better SSIM in contrast to Median Filter. Figure 9 shows the number of feature points. GLCM-CNN includes more number of feature points.

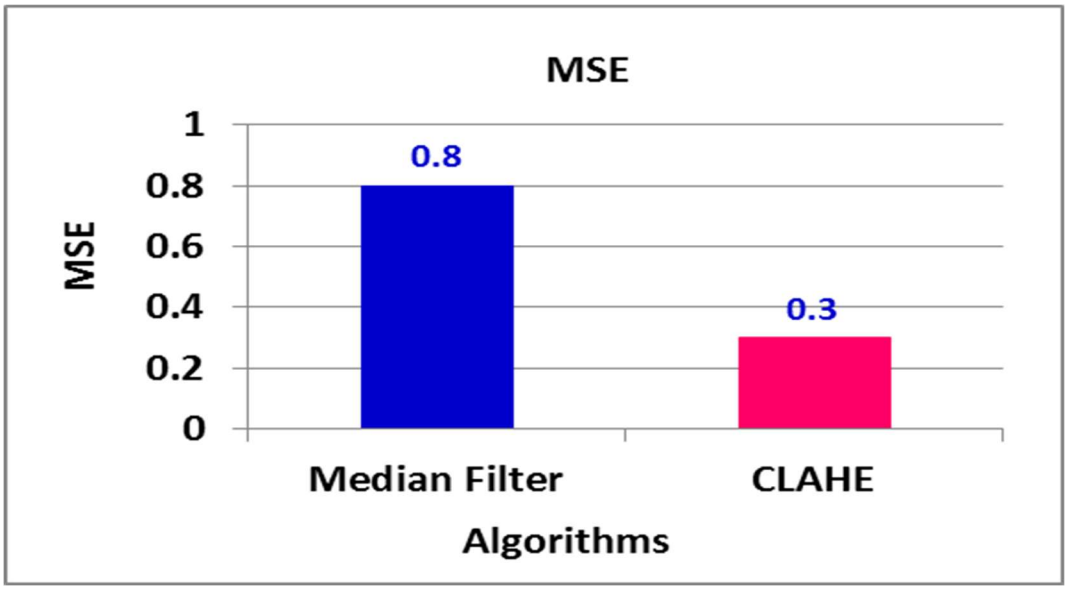

Figure 7: Mean Squared Error (MSE)

Vol. 21, No. 1, (2024)
ISSN: 1005-0930

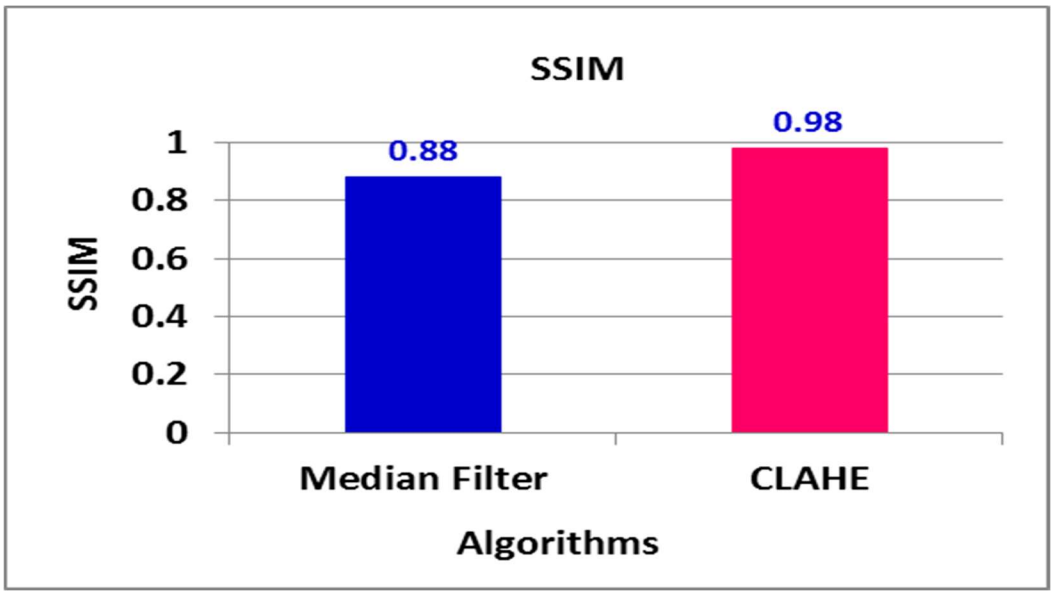

Figure 8: Structural Similarity Index Measure (SSIM)

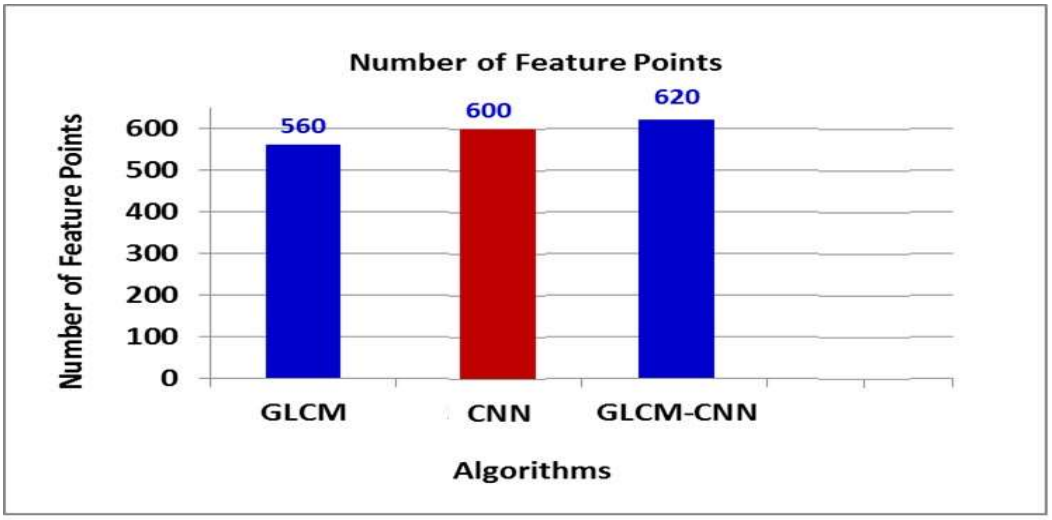

Figure 9: Number of Feature Points

Figure 10 gives the Accuracy. It is seen that without feature extraction, RF, CNN and CNN_RF offer 9%, 6% and 2% lesser Accuracy in contrast to the proposed CNN_XGB scheme. With feature extraction, it is seen that the proposed CNN_XGB offers 8%, 6% and 4% better accuracy when compared to RF, CNN and CNN_RF respectively.

Figure 11 gives the Precision. It is seen that without feature extraction, RF, CNN and CNN_RF offer 9%, 6% and 2% lesser Precision in contrast to the proposed CNN_XGB scheme. With feature extraction, it is seen that the proposed CNN_XGB offers 7%, 5% and 3% better Precision when compared to RF, CNN and CNN_RF respective.

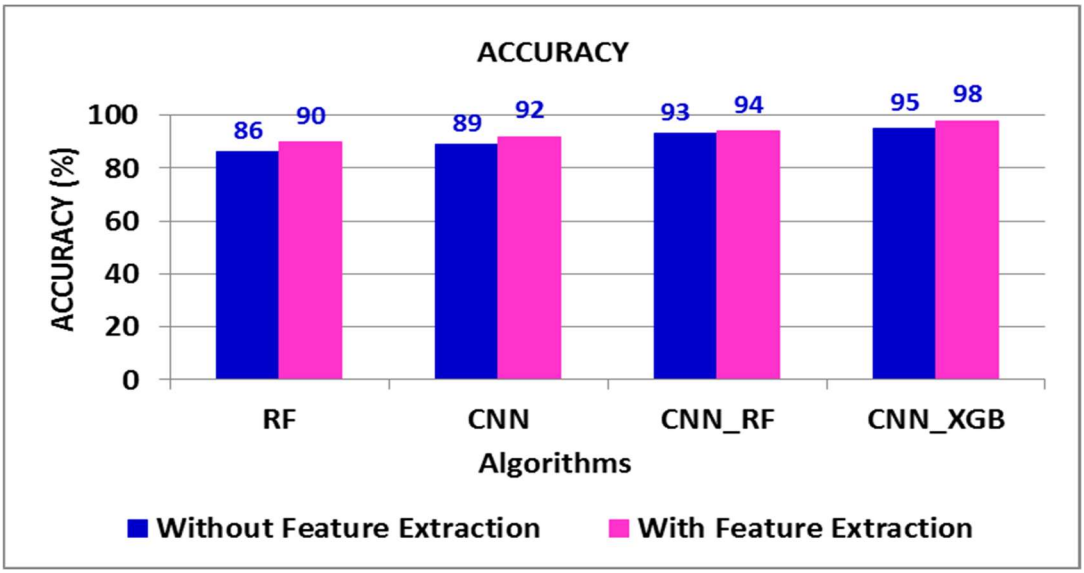

Figure 10: Accuracy

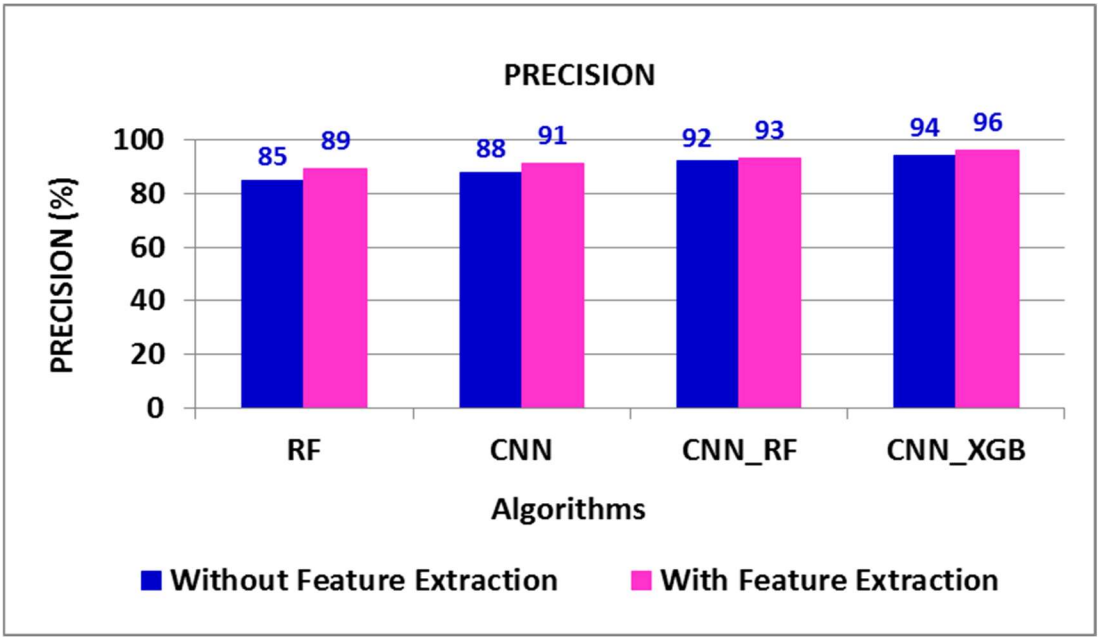

Figure 11: Precision

Vol. 21, No. 1, (2024)
ISSN: 1005-0930

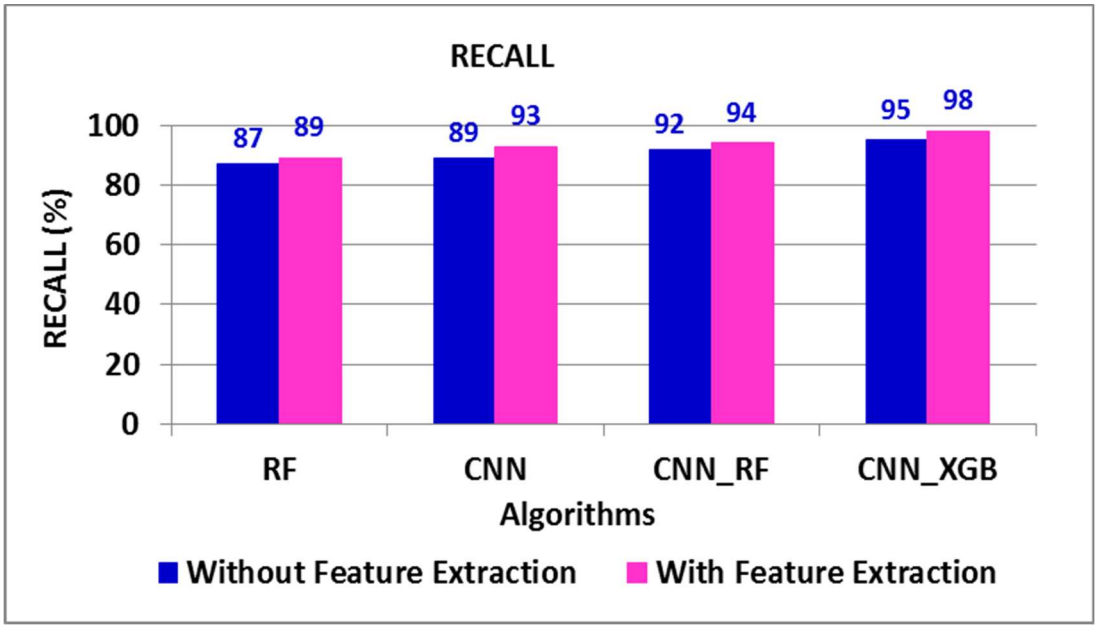

Figure 12: Recall

Figure 12 gives the Recall. It is seen that without feature extraction, RF, CNN and CNN_RF offers 8%, 6% and 3% lesser Recall in contrast to the proposed CNN_XGB scheme. With feature extraction, it is seen that the proposed CNN_XGB offers 9%, 5% and 4% better Recall when compared to RF, CNN and CNN_RF respectively.

Figure 13 gives the F-Measure. It is seen that without feature extraction, RF, CNN and CNN_RF offers 8%, 5% and 2% lesser F-Measure in contrast to the proposed CNN_XGB scheme. With feature extraction, it is seen that the proposed CNN_XGB offers
10%, 6% and 3% better F-Measure when compared to RF, CNN and CNN_RF respectively.

Vol. 21, No. 1, (2024)
ISSN: 1005-0930

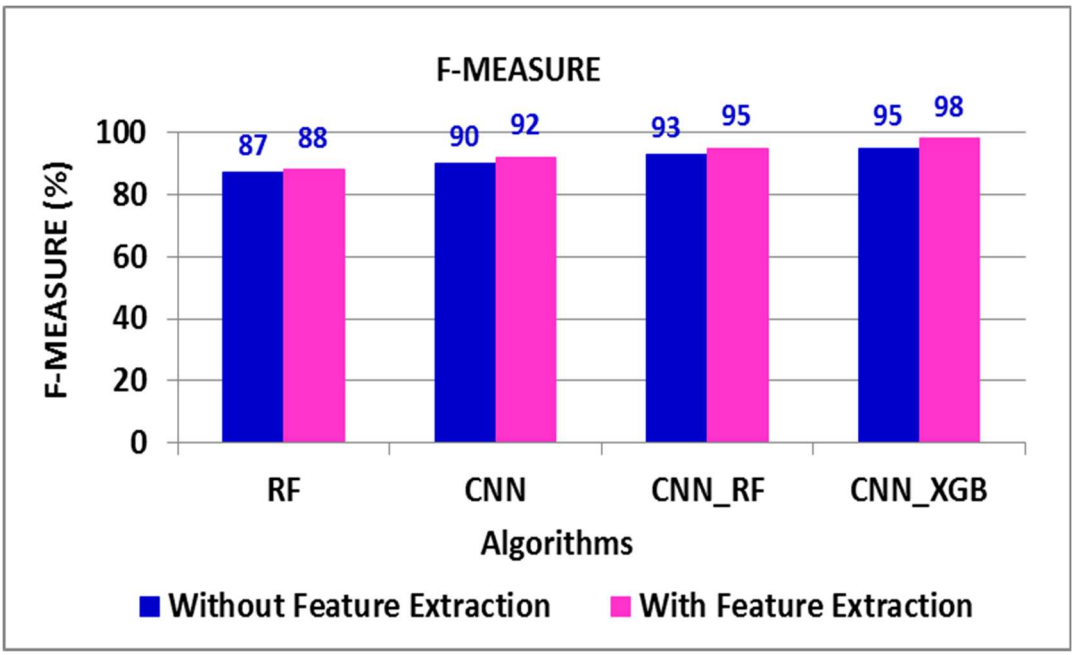

Figure 13: F-Measure

7. CONCLUSION

In this paper, a DL-based approach is proposed. Image pre-processing is done using Median Filter (MF) and CLAHE, while features are found using GLCM and CNN. Images are classified using RF and XGBoost. The proposed CNN_XGB scheme offers better results in terms of Accuracy, Precision, Recall and F-Measure in contrast to RF, CNN and CNN_RF.

REFERENCES

1. A.Subasi, A. Ahmed, E. Aličković and A. R. Hassan, "Effect of photic stimulation for migraine detection using random forest and discrete wavelet transform". Elsevier, Biomedical signal processing and control. (2019), vol. 49, pp231-239.
2. R. J. S. Raj, S. J. Shobana, I. V. Pustokhina, D. A. Pustokhin, D.Gupta and K. Shankar, "Optimal feature selection-based medical image classification using deep learning model in internet of medical things". IEEE, Access, (2020), vol.8, 58006-58017.
3. S. Liang, H. Liu, Y. Gu, X. Guo, Li. H, L.Li, Z. Wu, M.Liu and L. Tao. "Fast automated detection of COVID-19 from medical images using convolutional neural networks". Communications Biology, (2021), 4(1), pp1-13.

4. C. L. Chowdhary and D. P. Acharjya, "Segmentation and feature extraction in medical imaging: a systematic review". Elsevier, Procedia Computer Science, (2020), vol.167, pp 26-36.
5. Y. Oh, S. Park and J. C. Ye. "Deep learning COVID-19 features on CXR using limited training data sets". IEEE Transactions on medical imaging, vol.39, (2020). 2688-2700.
6. C. Sohrabi, Z. Alsafi, N. O'neill, M. Khan, A. Kerwan, A. A. Jabir, C. losifidis and R. Agha. "World Health Organization declares global emergency: A review of the 2019 novel coronavirus (COVID - 19)". International journal of surgery, (2020), vol.76, pp 71-76.
7. https://www.who.int/publications/m/item/weekly-epidemiological-update-on-covid-19---29-june-2021.
8. T. L. Sandri, J. Inoue, J. Geiger, J. M. Griesbaum, C. Heinzel, M. Burnet, R.Fendel, P.G.Kremsner, J. Held and A. Kreidenweiss. "Complementary methods for SARS-CoV-2 diagnosis in times of material shortage". Scientific reports, (2021), 11(1), pp 1-8.
9. M.Elsharkawy, A. Sharafeldeen, F. Taher, A. Shalaby, A. Soliman, A. Mahmoud,... and A. E. Baz. "Early assessment of lung function in coronavirus patients using invariant markers from chest X-rays images". Scientific Reports, (2021), 11(1), pp1-11.
10. B. E. Bejnordi, M. Veta, , P. J. V. Diest, B. V. Ginneken, N. Karssemeijer, G. Litjens,... and R. Venancio. "Diagnostic assessment of deep learning algorithms for detection of lymph node metastases in women with breast cancer". Jama, CAMELYON16 Consortium. (2017), vol. 318(22), 2199-2210.
11. J. Amin, M. Sharif, M. Yasmin and S. L. Fernandes. "Big data analysis for brain tumor detection: Deep convolutional neural networks". Elsevier, Future Generation Computer Systems, (2018), vol. 87, pp 290-297.
12. L.A.P. Romay, F. Cedrón, A. Pazos and A.B. P. Pazos. "Deep artificial neural networks and neuromorphic chips for big data analysis: pharmaceutical and bioinformatics applications". International journal of molecular sciences, (2016), vol.17(8), 1313.
13. E. Goceri and N.Goceri. "Deep learning in medical image analysis: recent advances and future trends". Research Gate, International Conferences CGVCVIP. (2017),
14. G. Litjens, T. Kooi, B. E. Bejnordi, A. Setio,… and C. I. Sánchez. "A survey on deep learning in medical image analysis". Medical image analysis, (2017), vol.42, pp 60-88.
15. K. Elasnaoui, Y. Chawki and A. Idri. "Automated methods for detection and classification pneumonia based on x-ray images using deep learning. Research Gate, In Book: In Artificial intelligence and blockchain for future pcybersecurity applications, (2021), pp. 257-284.
16. Z. Yao, X. Hu, X. Liu, W. Xie, Y. Dong, H. Qiu,... and J. Zhuang "A machine learning-based pulmonary venous obstruction prediction model using clinical data and CT image". International Journal of Computer-Assisted Radiology and Surgery, (2021),vol.16(4), pp 609-617.
17. A. Bhandary, G.A. Prabhu, V. Rajinikanth, K.P. Thanaraj, S.C. Satapathy, D.E. Robbins,... and N.S.M. Raja, "Deep-learning framework to detect lung abnormality–A study with chest

X-Ray and lung CT scan images". Elsevier. Pattern Recognition Letters, (2020), vol.129, pp 271-278.

18. M. Kuchana, A.Srivastava, R. Das, J. Mathew, A. Mishra and K. Khatter. "AI aiding in diagnosing, tracking recovery of COVID-19 using deep learning on Chest CT scans". Multimedia tools and applications, (2021), vol. 80(6), pp 9161-9175.
19. A.S. Joaquin. "Using deep learning to detect pneumonia caused by nCoV-19 from X-ray images". https://towardsdatascience.com/using-deep-learning-to-detect-ncov-19-from-x-ray-images-1a89701d1acd, (2020).
20. M. Heidari, S. Mirniaharikandehei, A. Z. Khuzani, G. Danala, Y. Qiu and B. Zheng. "Improving the performance of CNN to predict the likelihood of COVID-19 using chest X-ray images with preprocessing algorithms". International journal of medical informatics, (2020), vol. 144, 104284.
21. D. Wang, J. Mo, G. Zhou, L. Xu, and Y. Liu. "An efficient mixture of deep and machine learning models for COVID-19 diagnosis in chest X-ray images". PLoS ONE, (2020), vol.15(11), e0242535.
22. H. Alshazly, C. Linse, M. Abdalla, E. Barth and T. Martinetz. "COVID-Nets: deep CNN architectures for detecting COVID-19 using chest CT scans". PeerJ Computer Science, (2021), vol. 7, e655, pp1-40.
23. M. F. Aslan, M. F. Unlersen, K. Sabanci and A. Durdu, "CNN-based transfer learning-BiLSTM network: A novel approach for COVID-19 infection detection". Elsevier, Applied Soft Computing, (2021), vol. 98, 106912.
24. A. Bhattacharyya, D. Bhaik, S. Kumar, P. Thakur, R. Sharma and R. B. Pachori, "A deep learning based approach for automatic detection of COVID-19 cases using chest X-ray images". Biomed Signal Process and Control, (2022), vol.71, 103182.
25. W. Salama and M. Aly, "Framework for COVID-19 segmentation and classification based on deep learning of computed tomography lung images". Journal of Electronic Science and Technology, (2022), vol. 20(3), 100161.
26. S. Aslani and J. Jacob. "Utilisation of deep learning for COVID-19 diagnosis". Elsevier, Clinical Radiology, (2023), vol. 78(2), pp 150-157.
27. M. Constantinou, T. Exarchos, A. Vrahatis and P. Vlamos. "COVID-19 Classification on Chest X-ray Images Using Deep Learning Methods". International Journal of Environmental Research and Public Health, (2023), vol.20(3), 2035.
28. E.D. Pisano, S. Zong, B. M. Hemminger, M. DeLuca, R. E. Johnston, K. Muller and S. M. Pizer. "Contrast limited adaptive histogram equalization image processing to improve the detection of simulated spiculations in dense mammograms". Journal of Digital imaging, (1998), vol. 11(4), pp 193-200.
29. T. K. Ho. "Random decision forests". Proceedings of 3rd international conference on document analysis and recognition, IEEE, (1995), vol. 1, pp. 278-282.

30. T. Hastie, R. Tibshirani and J. Friedman. "The elements of statistical learning: Data Mining, Inference, and Prediction. 2nd edition, Springer series in statistics, (2010), vol. 66(4), pp. 1309-1315.
31. L. Huang, Y. Li, S. Chen, Q. Zhang, Y. Song, J. Zhang, and M. Wang "Building safety monitoring based on extreme gradient boosting in distributed optical fiber sensing". Elsevier, Optical Fiber Technology, (2020), vol. 55, 102149.
32. D. Yang , C. Martinez , L. Visuña , H. Khandhar, C. Bhatt, and J. Carretero, "Detection and analysis of COVID-19 in medical images using deep learning techniques". Journal of Scientific Reports, (2021), vol. 11, 19638
33. S. Guefrechi,M. B. Jabra, A. Ammar, A. Koubaa and H.Hamam. " Deep learningbased detection of COVID-19 from chest X-ray images, Springer Nature, (2021), vol. 80(21-23), 31803-31820.
34. Isa A. Computational intelligence methods in medical image-based diagnosis of COVID-19 infections. Computational Intelligence Methods in COVID-19: Surveillance, Prevention, Prediction and Diagnosis. Springer, Singapore, pp 251–270
35. www.covid19.who.int /WHO Coronavirus (COVID-19) Dashboard
36. S. Guefrechi, M. B. Jabra, A.Ammar, A. Koubaa, and H.Hamam "The Deep learning based detection of COVID-19 from chest X-ray images". Multimedia tools and applications journal, springer, (2021) 80:31803–31820
37. B.Hu , H. Guo , P. Zhou , Z. L. Shi , " Characteristics of SARS-CoV-2 and COVID-19", Nat Rev Microbiol, Springer, (2021),19(3, pp141-154.
38. P. Ndajah, H. Kikuchi, M. Yukawa, H. Watanabe and S. Muramatsu,"An Investigation On The Quality Of Denoised Images", International Journal Of Circuits, Systems And Signal Processing , (2011), Issue 4, vol. 5, pp 423 -434.
39. Z. Gao, Y. Xu, C. Sun, X. Wang, Y. Guo, S. Qiu, and K. Ma, "A systematic review of asymptomatic infections with COVID-19, Journal of Microbiol Immunol Infect. Elsevier, (2021), 54(1): 12–16.